The Geological Society of America
Memoir 215

Surface geophysics, Edwards and Trinity Aquifers, central Texas

Mustafa Saribudak*
Environmental Geophysics Associates, 2000 Cullen Avenue, #7, Austin, Texas 78757, USA

ABSTRACT

Geophysical methods have been an important component of effective hydrogeologic investigations over the Edwards and Trinity Aquifers in central Texas. Various electrical and electromagnetic methods have been used to map stratigraphy and geologic structure and to locate buried karst features. Geophysical methods can also characterize faults and fractures in the Balcones fault zone. Six case studies across three segments (San Antonio, Barton Springs, and Northern segments) of the Edwards Aquifer show that the locations of buried caves and sinkholes, on all three segments, are best defined using a combination of two- and three-dimensional resistivity imaging and natural potential (self-potential) methods. Localization and characterization of the Haby Crossing and Mount Bonnell faults, which are known to be the most significant faults in the Balcones fault zone, are best accomplished by integrating multiple geophysical methods (e.g., electrical resistivity, natural potential, magnetic, ground-penetrating radar, conductivity, and seismic refraction tomography). It is noted, however, that other karstic regions could respond differently to different geophysical methods and require different primary geophysical methods.

INTRODUCTION

Karst aquifers are characterized by a network of conduits and caves formed by chemical dissolution, allowing for rapid and often turbulent water flow. Karst features, such as caves, sinkholes, springs, and sinking streams, are difficult to properly characterize with traditional invasive methods such as drilling and trenching. Thus, karst environments are one of the most challenging landscapes to characterize in terms of groundwater, geotechnical engineering, and environmental issues. Geophysical methods can provide a karst reconnaissance survey guiding borings and detailed focused studies of complex karst landscapes. Multiple geophysical methods are often used to provide complementary data sets that are integrated to meet the objectives of karst investigations. The geophysical information can be used to locate caves and sinkholes in the subsurface, quantify hazard estimates for structures being planned over karstic landscapes, explore groundwater resources, and characterize geologic structure. Thus, geophysical data can greatly reduce hydrogeological knowledge gaps and can improve our understanding of karst flow systems.

SURFACE GEOPHYSICAL METHODS

Geophysical methods are powerful tools with which to explore the subsurface. The range of applications includes hydrological and hydrogeological characterization, locating voids and karstic features, soil characterization, and

*ega@pdq.net

Saribudak, M., 2019, Surface geophysics, Edwards and Trinity Aquifers, central Texas, *in* Sharp, J.M., Jr., Green, R.T., and Schindel, G.M., eds., The Edwards Aquifer: The Past, Present, and Future of a Vital Water Resource: Geological Society of America Memoir 215, p. 267–281, https://doi.org/10.1130/2019.1215(23).

TABLE 1. TRADITIONAL GEOPHYSICAL METHODS USED IN CHARACTERIZING KARSTIC FEATURES AND FAULTS

Method	Measured parameter
Resistivity	Earth resistance (Ω·m)
Natural potential (NP)	Electrical potentials (mV)
Ground-penetrating radar (GPR)	Dielectric constant
Conductivity	Earth conductivity (mS/m)
Gravity	Gravity pull (mGal)
Magnetic	Magnetic field (nanoTesla)
Induced polarization	Polarization voltages or frequency (ms)
Seismic	Travel times of reflected/refracted waves (velocity in m/s)

contamination assessment. Two-dimensional (2-D) and three-dimensional (3-D) resistivity imaging, natural potential (NP), electromagnetic (EM), gravity, and magnetic methods are the most used, while other technologies, such as seismic refraction with multichannel analysis of surface waves (MASW), have grown more popular over recent decades. The available techniques are characterized by different depths of penetration and resolution capabilities, from centimeters to kilometers. For this reason, there is motivation by the scientific community to integrate multiple geophysical methods to detect and characterize the subsurface by relying on the analysis of different physical properties (Table 1).

Geophysical methods have been an important component of effective hydrogeologic investigation of the Edwards Aquifer in central Texas. Geophysical surveys that employ a combination of electrical and EM methods have been used to map stratigraphy, geologic structure, and depth to the water table in major aquifer systems (e.g., Fitterman and Stewart, 1986; Connor and Sandberg, 2001). Geophysical methods have also been used to delineate the locations of karst features (Green et al., 2015; Gary et al., 2013; Shah et al., 2008; Smith et al., 2005; Blome et al., 2008; Prikryl et al., 2007; Saribudak et al., 2010, 2012a, 2012b, 2013; Saribudak, 2011, 2015, 2016; Saribudak and Hauwert, 2017).

Geophysical surveys over three segments of the Edwards Aquifer are presented in this chapter: two case studies (1 and 2) from the San Antonio segment; three case studies (3, 4, and 5) from the Barton Springs segment; and one case study (6) from the Northern segment (Fig. 1). The intent of this chapter is to show how integrated geophysical methods could provide significant information on the hydrostratigraphy of the Edwards Aquifer, in general, and on karstic features, faults, and fractures within the Balcones fault zone, in particular.

GEOPHYSICAL CASE STUDIES

The six case studies presented here demonstrate that geophysical methods can be used effectively to locate faults and karstic features (caves and sinkholes) and map stratigraphy and geologic structure of the Edwards Aquifer, which is bounded by the Balcones fault zone (see Fig. 1).

San Antonio Segment

Survey 1: School Cave

A series of voids was encountered during the installation of piers into the limestone of the Person Formation (Stein and Ozuna, 1996) for a construction project. In total, six boreholes were drilled at the site. These voids had a depth of ~4 m (15 ft) and appeared to be connected at depth. A combination of tape measure and video camera methods indicated that the cave extended as deep as 15 m. The cave was air-filled but wet. Following the discovery of the voids, geophysical surveys were conducted to evaluate the extent of the cave and the voids. The surveys included resistivity, NP, and ground-penetrating radar methods (Saribudak et al., 2012a). Four resistivity profiles with a spacing of 6 m (20 ft) separating the profiles were acquired across the pier locations and adjacent areas. Figure 2A displays one of the resistivity imaging profiles along with four borehole locations, three of which encountered the cave. It is important to note that the cave was characterized by high-resistivity (10,000 Ohm-m), medium-resistivity (750 Ohm-m), and low-resistivity (200 Ohm-m) values. The fourth borehole did not encounter a void. Figures 2B and 2C also show NP data and a pseudo–3-D resistivity image, which was created by combining four 2-D resistivity profiles. The NP data indicate a significant low NP anomaly where the cave is located.

The NP data (Fig. 2B) indicate a significant anomaly encompassing the locations of three pier locations where the cave was encountered. A 3-D resistivity plan view of the cave area in Figure 2C denotes three boreholes that encountered the void (red circle). Three borehole locations that did not encounter the cave are shown with yellow circles. Note that the boundaries of the cave defined by the borehole data include the low-resistivity values. The 3-D image of the resistivity data appears to define the geometry of the cave better than the 2-D resistivity data.

Survey 2: Haby Crossing Fault

Haby Crossing fault, which is located in eastern Medina County, Texas, is a significant fault within the Balcones fault zone with as much as ~90 m (300 ft) of displacement (Clark, 2000; Small and Clark, 2000). The fault has been characterized as a barrier to groundwater flow (Maclay and Land, 1988;

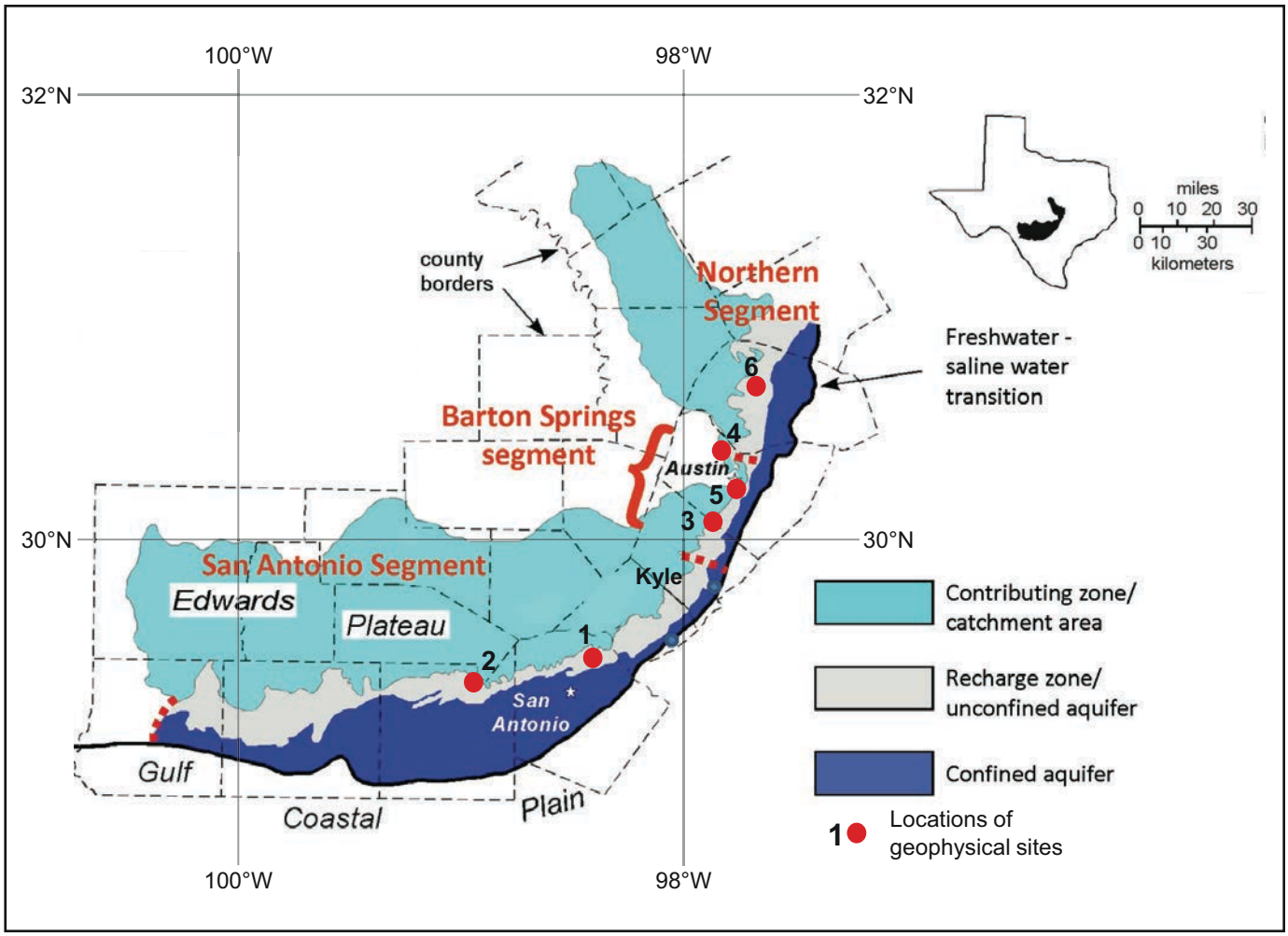

Figure 1. Location of geophysical sites across the three segments of the Edwards Aquifer (Musgrove and Banner, 2004).

Lindgren et al., 2004). Electrical resistivity, NP, ground conductivity (EM31), and magnetic surveys were conducted along a transect that crossed the Haby Crossing fault. The profile is within the Balcones fault zone and includes three transmission pole locations (numbered 80 through 82; see Fig. 3A). In general, it is hypothesized that fault deformation in the Balcones fault zone increases permeability within and near faults, with the exception of clay or shale smear (Ferrill and Morris, 2008). The goal of Saribudak et al. (2010) and this chapter was to characterize the Haby Crossing fault in terms of its dissolution features (voids), permeability, and mineralization content, and as well as its faulting signature.

Electrical resistivity, NP, ground conductivity, and magnetic data are shown in Figure 3. Electrical resistivity values vary between 2 and 10,000 Ohm-m. The depth of exploration of resistivity data is ~38 m (125 ft). The resistivity data indicate two faults locations at 207 m (680 ft) and 330 m (1080 ft), respectively. The fault at 207 m corresponds to the Eagle Ford Group rocks. Resistivity values of the Eagle Ford Group rocks vary from 2 to 150 Ohm-m, consistent with clay and weathered limestone. The fault at 330 m, which is the Haby Crossing fault, juxtaposes the Eagle Ford Group with the dolomitic member of Kainer Formation, which has a resistivity up to 10,000 Ohm-m. The dragging of low-resistivity units (blue in color) in the downthrown side of the Haby Crossing fault against the high-resistivity layers of the Kainer Formation denotes the fault location (Fig. 3A).

NP data across the Haby Crossing fault are illustrated in Figure 3B. The NP data indicate prominent karst anomalies such as voids and caves denoted with numbers 1, 2, and 3 on the NP profile. It is important to note that anomaly 1 occurs within the upper confining unit between two faults (see Fig. 3B). The NP anomaly across the Haby Crossing fault is quite distinct where NP values fall from 20 to –5 mV. Ground conductivity values vary from 80 mS/m at the south end of the profile to 20 mS/m across the first fault, and zero (0) mS/m across the Haby Crossing fault (Fig. 3C). This ground conductivity low is attributed

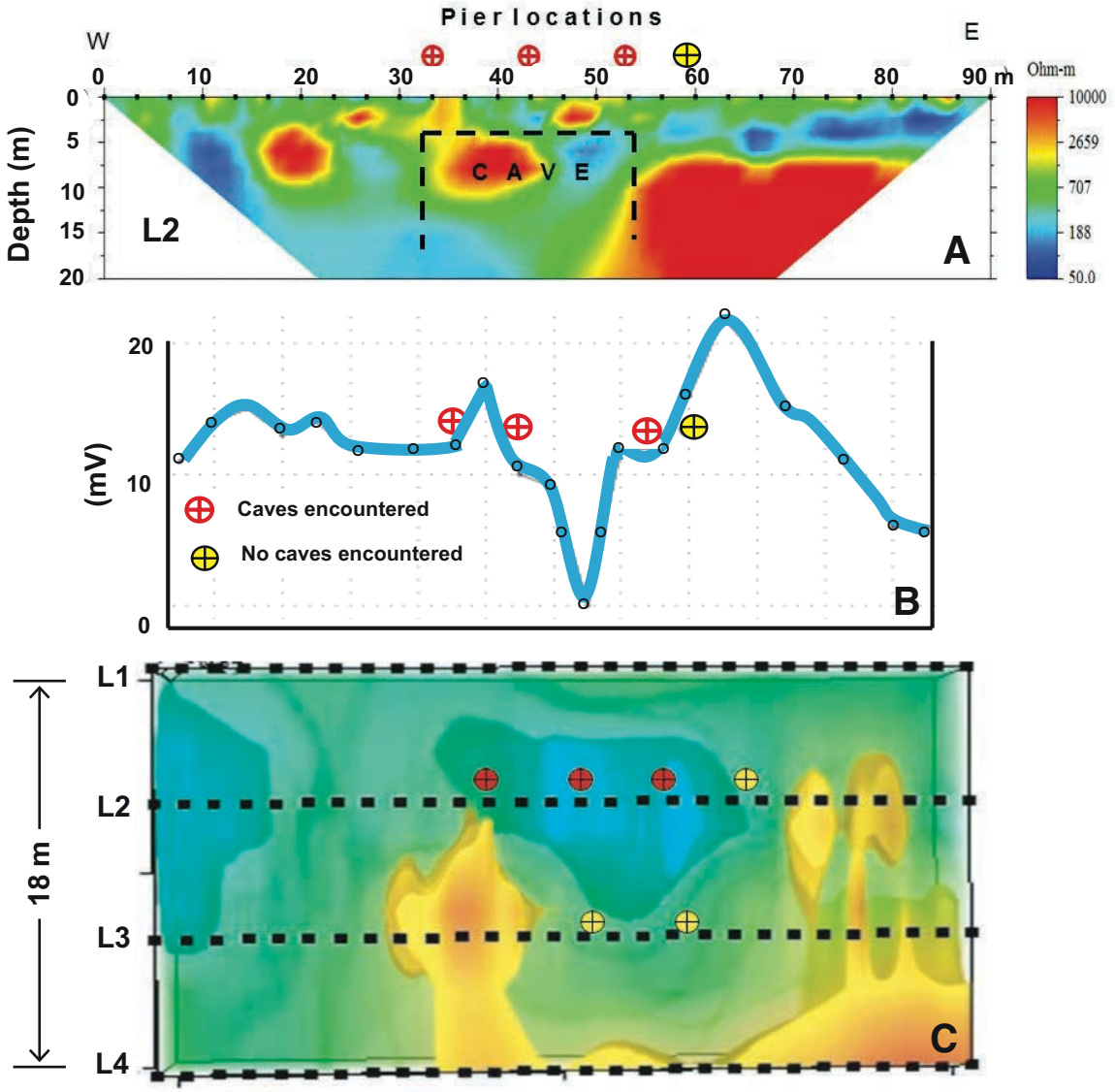

Figure 2. Geophysical survey results: (A) resistivity, (B) natural potential (NP), and (C) three-dimensional (3-D) top-view of resistivity data across the cave location. Note that resistivity values on the 3-D view (C) are much less than the resistivity profile L2 (A). This is probably due to the volume distribution of the resistivity values versus the area.

to the resistive dolomitic member of the Kainer Formation. The magnetic profile across the Haby Crossing fault is illustrated in Figure 3D. The prominent high magnetic anomaly is attributed to the Haby Crossing fault. The location of the high magnetic anomaly is well correlated with NP anomaly 2. Thus, the source for the magnetic anomaly could be due to a void or cave containing ferrous mineralization within the Haby Crossing fault plane.

In summary, the location of the Haby Crossing fault was discerned using each geophysical technique used in this study. In addition, the resistivity data indicated another fault to the south of the Haby Crossing fault. The presence of two faults appears to define a fault zone, the width of which is ~150 m (500 ft). The NP data indicate significant karst anomalies (voids, caves, conduits, fissures, etc.) within this fault zone. These results show that the fault zone includes voids, fractures, weathered limestones, and clay layers, all of which help to increase the vertical and horizontal permeability of the fault zone, with the exception of the clay confining units. With the presence of these karstic features, the Haby Crossing fault zone may enhance recharge of groundwater flow.

Barton Springs Segment

Survey 3A: Antioch Cave at Onion Creek

The next study area was located in the Barton Springs segment of the Edwards Aquifer, near Onion Creek and the City of

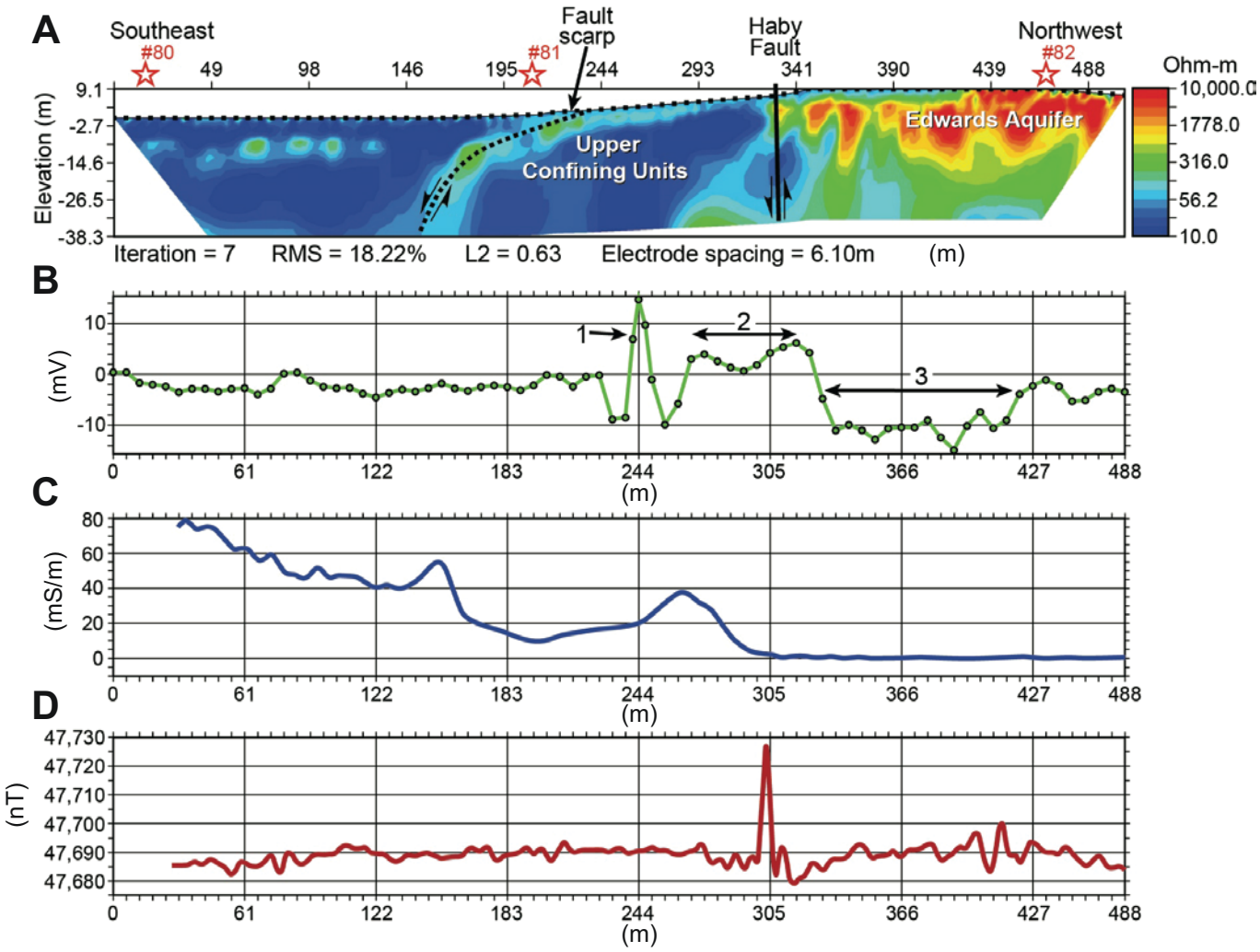

Figure 3. Geophysical survey results: (A) resistivity imaging, (B) natural potential (NP), (C) ground conductivity, and (D) magnetic data across the Haby Crossing fault. RMS error (root mean squared) is the statistical parameter that gives a difference between measured and calculated resistivity values (see text).

Buda. Electrical resistivity and NP surveys were conducted in the vicinity of Antioch Cave, the largest known recharge feature in the bed of Onion Creek (Saribudak et al., 2012b). The geophysical surveys targeted geologic units, surface geologic mapping, the throw of the individual fault(s), and possible karstic features within the fault zone. Understanding the geometry of the geologic units and faulting has implications for the extent of the recharge zone boundary and the permeability architecture of the recharge features and aquifer in the study area. The uninterpreted resistivity and geologically interpreted resistivity data that were collected along the northern bank of Onion Creek are provided in Figure 4.

The location of the Georgetown Formation outcrop is interpreted as the green color in the western part of the profile. Underlying the Georgetown Formation, there are the Edwards Group units, which are displayed with yellow and red colors. The contact between the Edwards Group units and the Georgetown Formation appears to be quite well defined. However, this conformity disappears at ~110 m (360 ft) to the east of the first interpreted fault. Furthermore, there is a chaotic disturbed zone in the subsurface between stations 110 m (360 ft) and 150 m (490 ft). In order to explain the resistivity structure of the geological units, a second fault, predicted by the resistivity data, was placed at station 145 m (Fig. 4), which juxtaposes the Georgetown Formation and Edwards Group units with the Del Rio Formation.

There is a relatively uniform resistivity section between stations 162 m (532 ft) and 232 m (761 ft) where a low-resistivity unit (Del Rio Formation) is observed at 4 m below ground surface. It should be noted that the surface geology between stations 162 m (532 ft) and 232 m (761 ft) is identified as alluvium. Resistivity data indicate a significant fault at station 245 m (820 ft). Resistivity data indicate that the fault juxtaposes the Del Rio

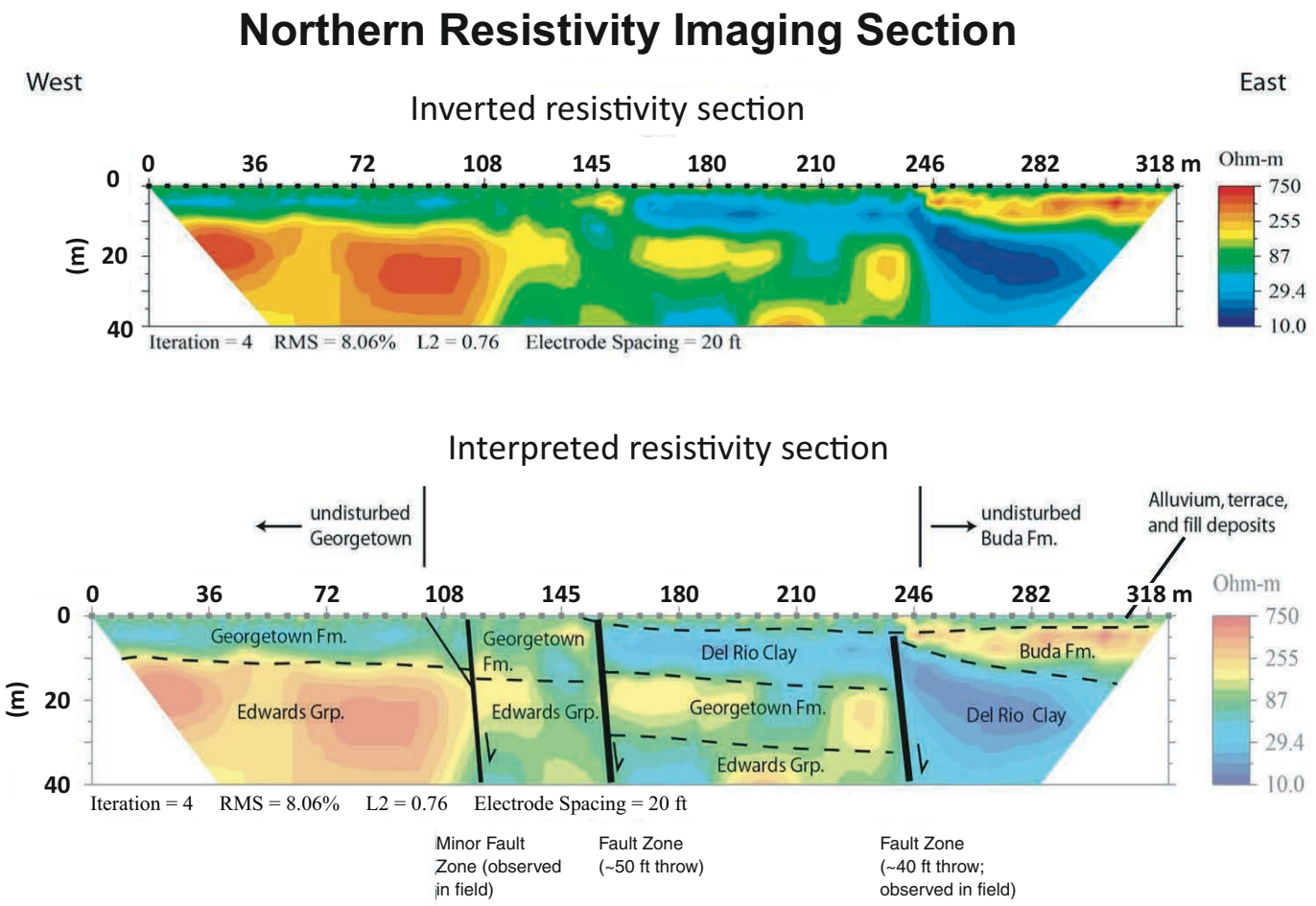

Figure 4. Inverted and interpreted resistivity data along the northern bank of Onion Creek. RMS error (root mean squared) is the statistical parameter that gives a difference between measured and calculated resistivity values (see text). 20 ft = 6 m.

Formation against the Buda Limestone. The Del Rio Formation has a thickness of ~6 m (20 ft) on the upthrown side of the fault (northwest direction), whereas it has an apparent thickness of 30 m (100 ft) on the downthrown side. In addition, the Del Rio Formation appears to be deformed and folded along the fault plane. This deformation could account for the increase in apparent thickness.

Survey 3B: Sinkhole at Onion Creek

The NP profile surveyed across an apparent sinkhole in the bed of Onion Creek between northern transect stations 110 m (360 ft) and 115 m (380 ft). This location was indicated on the geological map of the site as "suspected sinkhole" (Saribudak et al., 2012b). The NP data indicate a significant negative anomaly (~–8 mV) between stations 6 m (20 ft) and 18 m (60 ft), which corresponds to the sinkhole location (Fig. 5). This NP anomaly is hypothesized to result from recharge to the sinkhole. In summary, integrated geophysical results combined with the geological data indicate that geophysical methods can be used successfully to map stratigraphy and structure (faults and fractures) over the Edwards Aquifer and the overlying geological formations such as the Del Rio Formation and Buda Limestone.

Survey 4: Barton Springs Pool Conduit at Main Barton Springs

The Main Barton Springs is a major discharge site for the Barton Springs segment of the Edwards Aquifer in Zilker Park, Austin, Texas. Barton Springs actually consist of at least four springs. The Main Barton Springs and several outlets along a cave, several fissures, and gravel-filled solution cavities on the floor of the pool west of the fault discharge into the Barton Springs pool (Hauwert et al., 2004; Hauwert, 2009). The surface geology of the Main Barton Springs area includes Edwards Aquifer units (regional dense and leached collapsed members) and the Georgetown Formation (Hauwert, 2009). The Barton Springs fault juxtaposes the Edwards Group units against the Georgetown Formation.

Multiple geophysical surveys were conducted in the vicinity of the Barton Spring Pool in Austin, Texas (Saribudak et al., 2013; Saribudak and Hauwert, 2017). Electrical resistivity, NP,

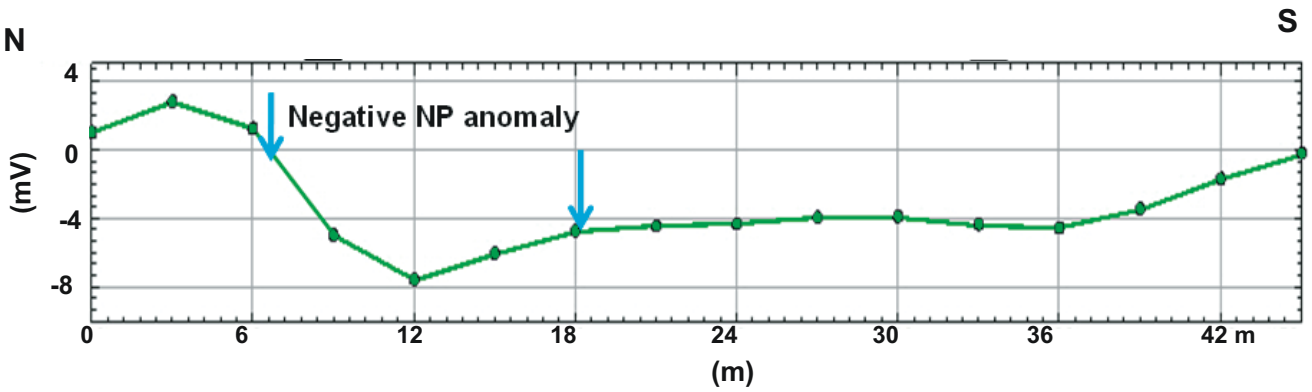

Figure 5. Natural potential (NP) data across the suspected sinkhole location on the bed of Onion Creek. The Antioch Cave entrance is located ~45 m to the west of the NP profile.

induced polarization (IP), and tomographic seismic refraction surveys were conducted on an east-west transect along the southern fence boundary of the swimming pool at Zilker Park (for location, see site map of Fig. 6).

Geophysical results are provided in Figure 6. The resistivity data (Fig. 7A) indicate a significant low-resistivity anomaly (blue in color) at a depth of ~10 m (33 ft). The south gate entrance to Zilker Park is denoted on the profile for reference. The anomaly has a width of 10 m and appears to dip to the east. The low-resistivity anomaly is interpreted to be caused by a combination of water and/or clay associated with a karst conduit. The IP data illustrate a high IP anomaly (red in color) at the same location as the low-resistivity anomaly (Fig. 7B). The source of the IP anomaly could be due to clay formations and/or minerals such as sulfide particles. The seismic refraction data not only define the potential geological units (Edwards Aquifer units and Georgetown Formation), but also a fault-like anomaly where the resistivity and IP anomalies are observed (Fig. 7C). One of the significant results discovered from these surveys was the common geophysical anomaly that was observed on all geophysical profiles. The location of the Main Barton Springs that flow into the pool correlates with the location of the geophysical anomalies.

An additional four more E-W resistivity profiles were conducted parallel to profile L1 (Saribudak and Hauwert, 2017). A pseudo–3-D resistivity block diagram was constructed using five 2-D east-west resistivity profiles and is shown in Figure 8A. An NP profile, which was surveyed along profile L1, is also shown in Figure 8B. Note that the 3-D diagram indicates a well-defined low-resistivity zone where a high NP anomaly is located.

In summary, the results of all geophysical data suggest the presence of a conduit anomaly near the south gate entrance to the swimming pool, which is approximately aligned where the Main Barton Springs discharge to the Barton Springs swimming pool. The groundwater flow to the Main Barton Springs may follow the locations of the geophysical anomalies.

Survey 5: Mount Bonnell Fault

Geophysical surveys were conducted at three locations across the Mount Bonnell fault in the Balcones fault zone of central Texas (Saribudak, 2011, 2016); however, only one transect is discussed in this paper. The Mount Bonnell fault is a normal fault with hundreds of meters of throw. It forms the primary boundary between the Trinity and Edwards Aquifers. In the near surface, the fault juxtaposes the Upper Glen Rose Formation, consisting of interbedded limestone and marly limestone, against the Edwards Group, which is mostly limestone, on the eastern downthrown side.

Electrical resistivity, NP, and ground-penetrating radar data were collected at the Height Drive transect where the Mount Bonnell fault crosses Highway 360 in south Austin. Resistivity and NP surveys were conducted on grassy ground, whereas the ground-penetrating radar data survey was conducted on the asphalt next to the resistivity and NP transects (Saribudak, 2011, 2016). The resistivity data indicate a significant anomaly consisting of high and low resistivity between stations 80 m (260 ft) and 95 m (310 ft). The source for this anomaly is not known, but it could be a karst feature such as a clay-filled cave. The location of the fault based on the geological data was marked on the resistivity profile. The resistivity profile does not indicate an anomaly where it crosses the Mount Bonnell fault (Fig. 9A). This observation suggests that the Glen Rose units on the upthrown side have similar resistivity values as the Edwards Aquifer units in the near surface. However, the NP data show a significant anomaly across the known fault location (Fig. 9B).

The ground-penetrating radar data (Fig. 8C) show a significant amplitude contrast across the Mount Bonnell fault. The fault location defined using the seismic data corresponds to the NP data and geologic mapping of the fault. The Glen Rose Formation (low amplitudes indicated by blue, green, yellow, and brown colors in Fig. 9C) is juxtaposed with Edwards Aquifer units (high amplitudes of white and gray colors). In summary, the geophysical results corroborated the suspected karstic feature in the Glen

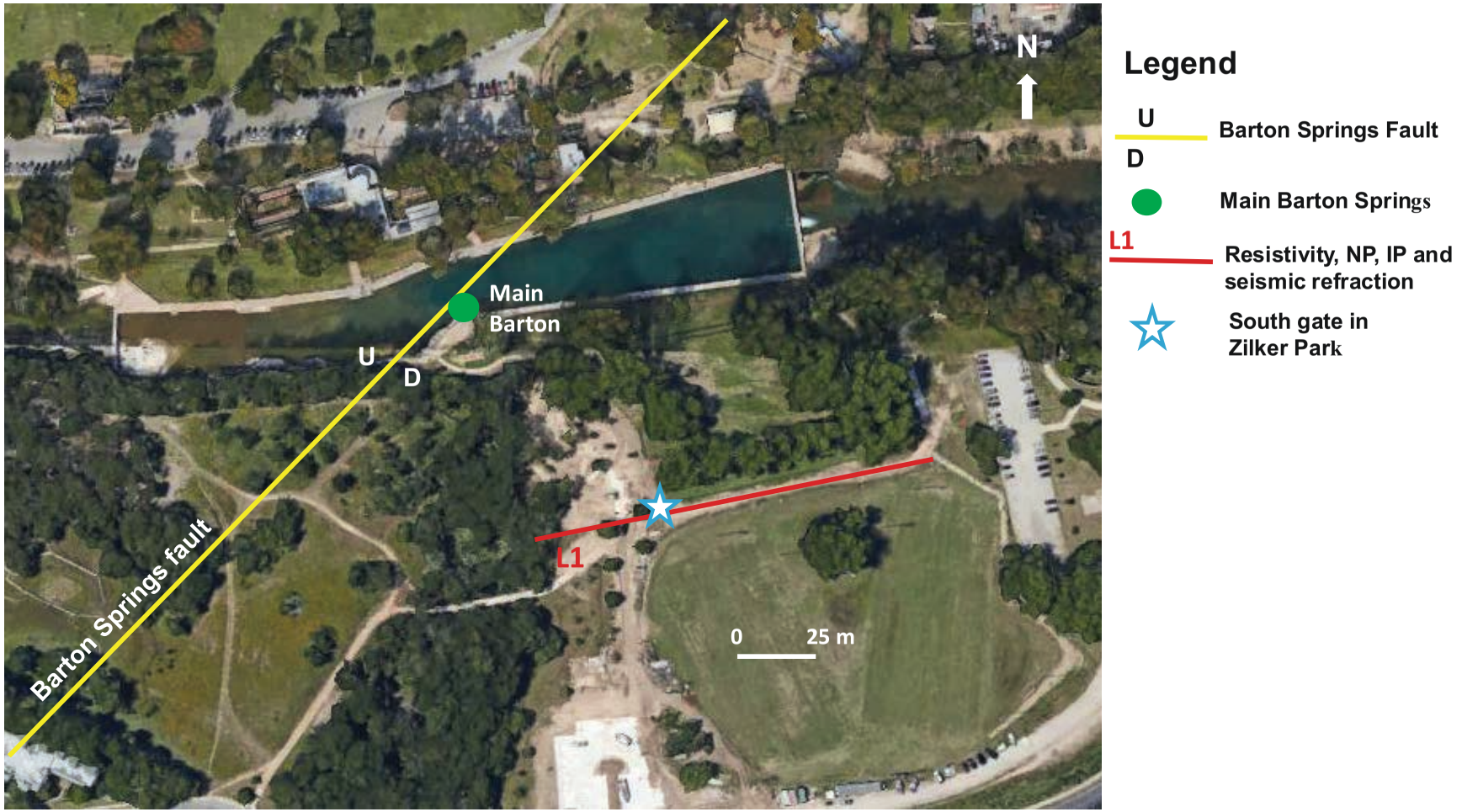

Figure 6. Resistivity, natural potential (NP), induced polarization (IP), and tomographic seismic refraction surveys were conducted along profile L1. Four more resistivity profiles parallel to profile L1 were surveyed but are not displayed in this figure (see Saribudak and Hauwert, 2017).

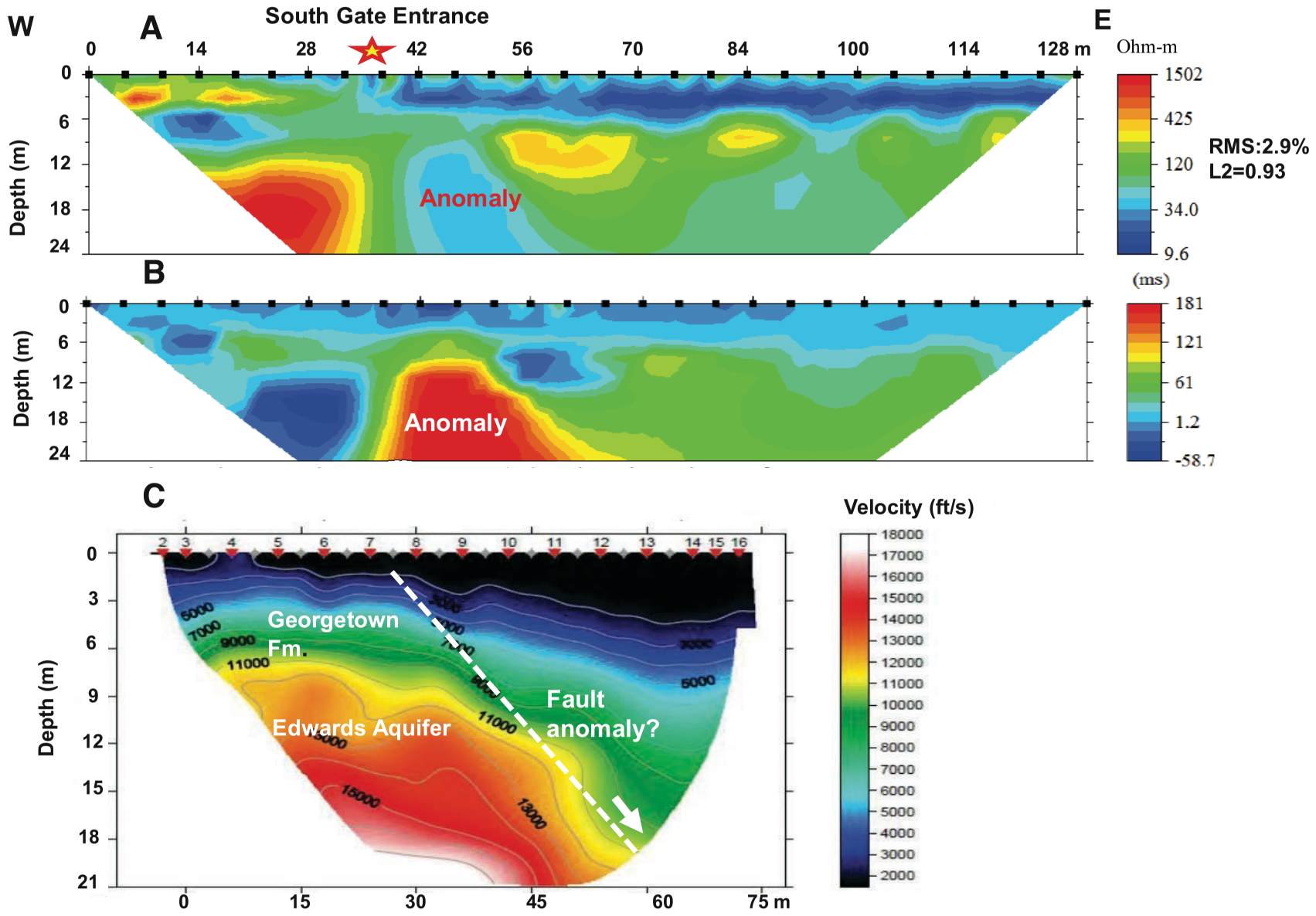

Figure 7. Geophysical survey results: (A) electrical resistivity, (B) induced polarization (IP), and (C) seismic refraction surveys at Barton Springs. Note the low-resistivity anomaly (A), high IP anomaly (B), and a fault-like seismic refraction anomaly (C). RMS error (root mean squared) is the statistical parameter that gives a difference between measured and calculated resistivity values (Fig. 7A). Velocity values of C correspond to 600 and 5500 m/s.

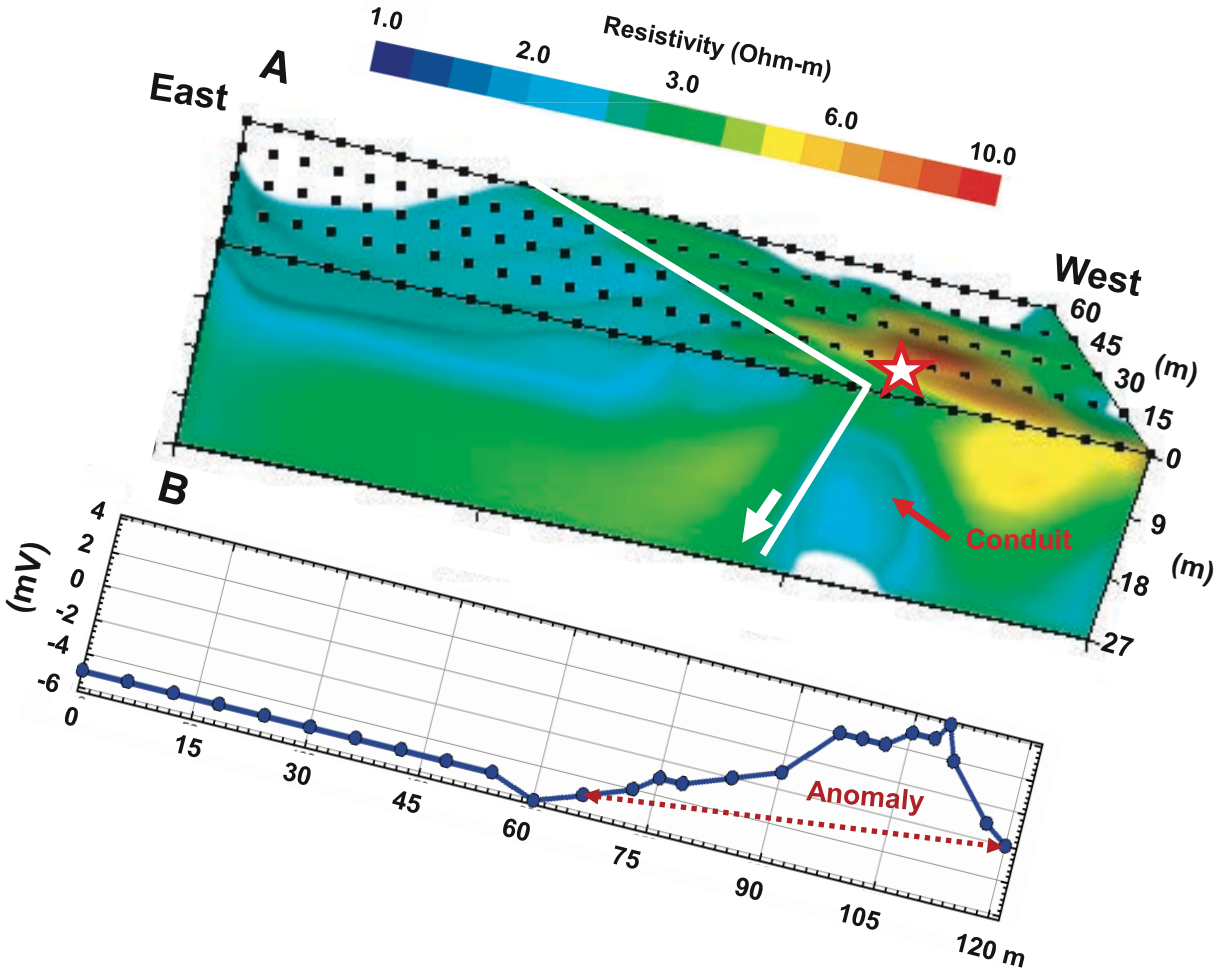

Figure 8. (A) Pseudo–three-dimensional (3-D) resistivity block and (B) natural potential (NP) data near the south gate entrance in the Zilker Park. The red star symbol shows the approximate location of the south gate entrance to the pool. Note that the direction of the figures was switched from west-to-east to east-to-west for proper illustration of the anomalies. The best hydrogeological view of the 3-D diagram was accomplished by tilting the 3-D block.

Rose Formation (Upper Trinity Aquifer) and Edwards Aquifer units and the mapped location of the Mount Bonnell fault.

Northern Segment

Survey 6: McNeil School at Austin

The City of Austin Watershed Protection Department performed a hydrogeologic investigation related to the design and construction of the Martin Hill Transmission Main on the Northern segment of the Edwards Aquifer recharge zone. Several karst features were identified by the City of Austin in the vicinity of the recharge zone. These features included a sinkhole/cave opening located behind McNeil High School; the McNeil Bat Cave, located on the east side of the high school; and two other caves (Weldon Cave, No Rent Cave) located west of the high school. Multiple geophysical surveys (electrical resistivity, NP, ground-penetrating radar data, magnetic, and ground conductivity) were performed across the site (Saribudak, 2015). In this paper, only resistivity and NP results along the McNeil Road are discussed (for location, see Fig. 10).

A combination of resistivity and NP data from the west side of the study area is provided in Figure 11. The resistivity data indicate a high-resistivity layer undulating under a low-resistivity layer along the profile. There is no striking anomaly along the resistivity data (Fig. 11A). However, the NP data (Fig. 11B) display a significant high anomaly, shown with a red font letter A, over a horizontal distance of 60 m with a magnitude of 50 mV.

Another combination of resistivity and NP data from the east side of the study area, where the McNeil High School is located, is shown in Figure 12. The resistivity data do not show any significant indication of a karstic feature (Fig. 12A). The NP data (Fig. 12B), however, clearly display a major anomaly between stations 121 m (397 ft) and 168 m (550 ft), which is denoted with the letter B. The maximum magnitude of this NP anomaly is 40 mV.

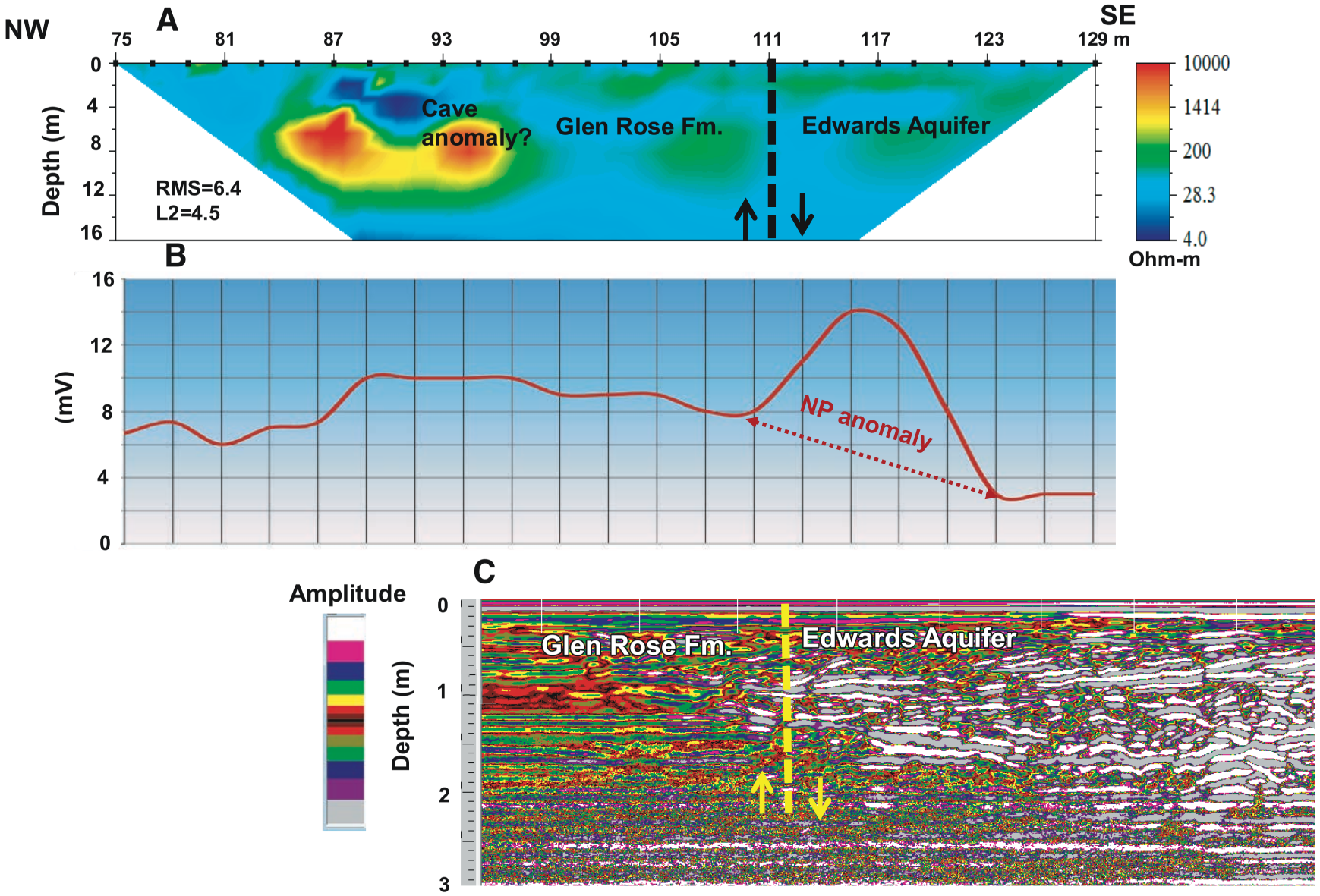

Figure 9. Geophysical survey results: (A) electrical resistivity, (B) natural potential (NP), and (C) GPR surveys at the Mount Bonnell fault at Height Drive on Highway 360 in south Austin, Texas. RMS error (root mean squared) in A is the statistical parameter that gives a difference between measured and calculated resistivity values.

In summary, during the months of summer and fall of 2014, major construction activity started on McNeil Road along the geophysical profile. Bulldozers excavated the water transmission line down to a depth of 6 m (20 ft) on McNeill Drive. Two caves were encountered at a depth of 5 m (16 ft) where the NP anomalies A and B are located. Pictures of the discovered caves are also included in Figures 11 and 12.

FUTURE TREND IN SURFACE GEOPHYSICS

Opinions concerning the effectiveness of these geophysical surveys are mixed, and geophysical techniques are not generally recognized as primary tools in karstic studies. However, recent advances in geophysical instruments have made surface geophysics a viable tool for characterization of the karstic Edwards and Trinity Aquifers. Data quality has improved with the advent of continuous data collection. Data are better processed and interpreted by new and improved software packages, which produce improved subsurface imaging and mapping. However, researchers looking to apply surface geophysics should be well versed in the geological knowledge of the subject area because efficient survey design and good geophysical data collection require adequate understanding of the local geology. With the advent of the digital communication, the dissemination of geophysical data has been widespread; thus, the exchange of geophysical information and related experiences will likely yield better applications and better results.

The introduction of unmanned aerial vehicles (UAVs) or drones has provided another technological breakthrough in surface geophysical surveying. UAVs are used for geophysical surveys by the mining industry, for offshore surveys, and for geological mapping by the oil and gas industry. The decreasing cost of flying drones will provide affordable and efficient performance for surface geophysical techniques over the sensitive areas of the Edwards/Trinity Aquifers, or in similar regions, with a low environmental impact.

CONCLUSIONS

Surface geophysical methods have been used extensively and successfully to locate buried sinkholes, caves, and conduits in and over the Edwards and Trinity Aquifers during the past 15 yr. Other applications include delineation and characterization of faults and fractures, hydrostratigraphy, and bedrock topography. One of the keys to this success has been the application of two or more integrated geophysical methods and incorporation of extensive geological information. It appears that the most successful geophysical methods for detecting karstic features in central Texas are the combination of resistivity imaging and NP methods, although different karstic regions might respond better to other surface geophysical methods than the Edwards/Trinity Aquifers.

ACKNOWLEDGMENTS

Most of these studies were borne out of a passionate curiosity to understand the geophysical signatures of the Edwards Aquifer's karstic features and their most significant faults. A research

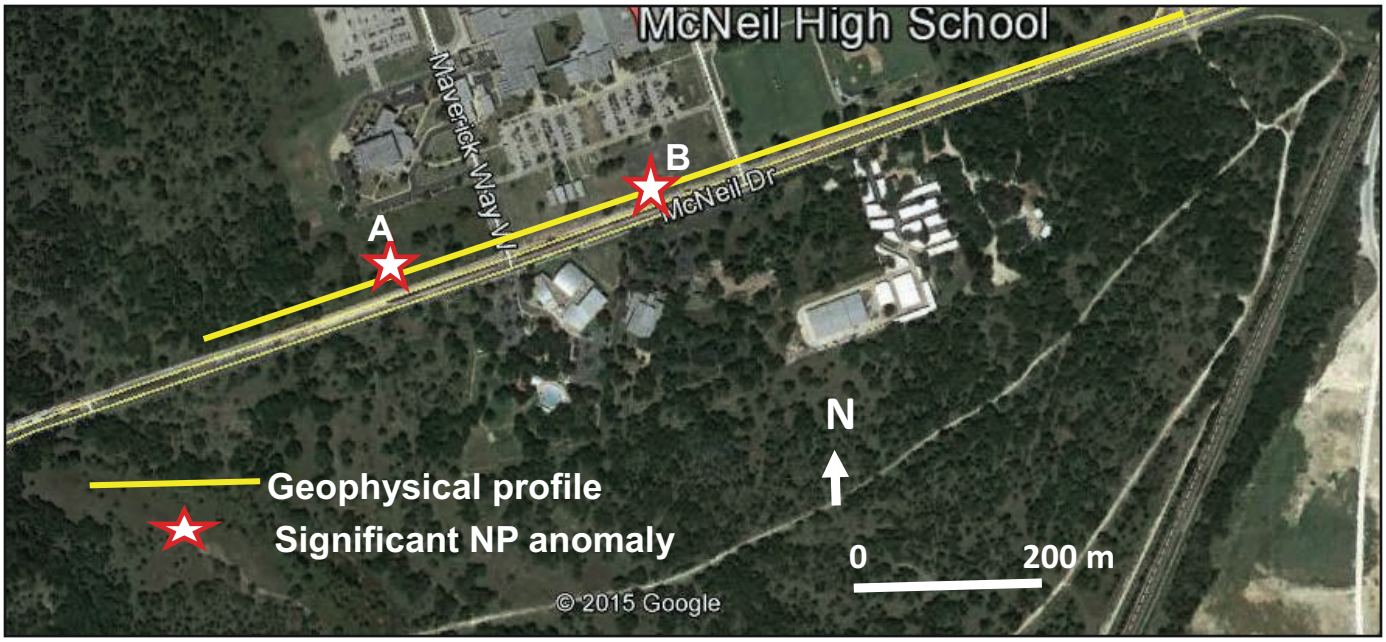

Figure 10. Site map showing the location of the geophysical profile near McNeil High School at McNeil Drive in northern Austin, Texas. NP—natural potential.

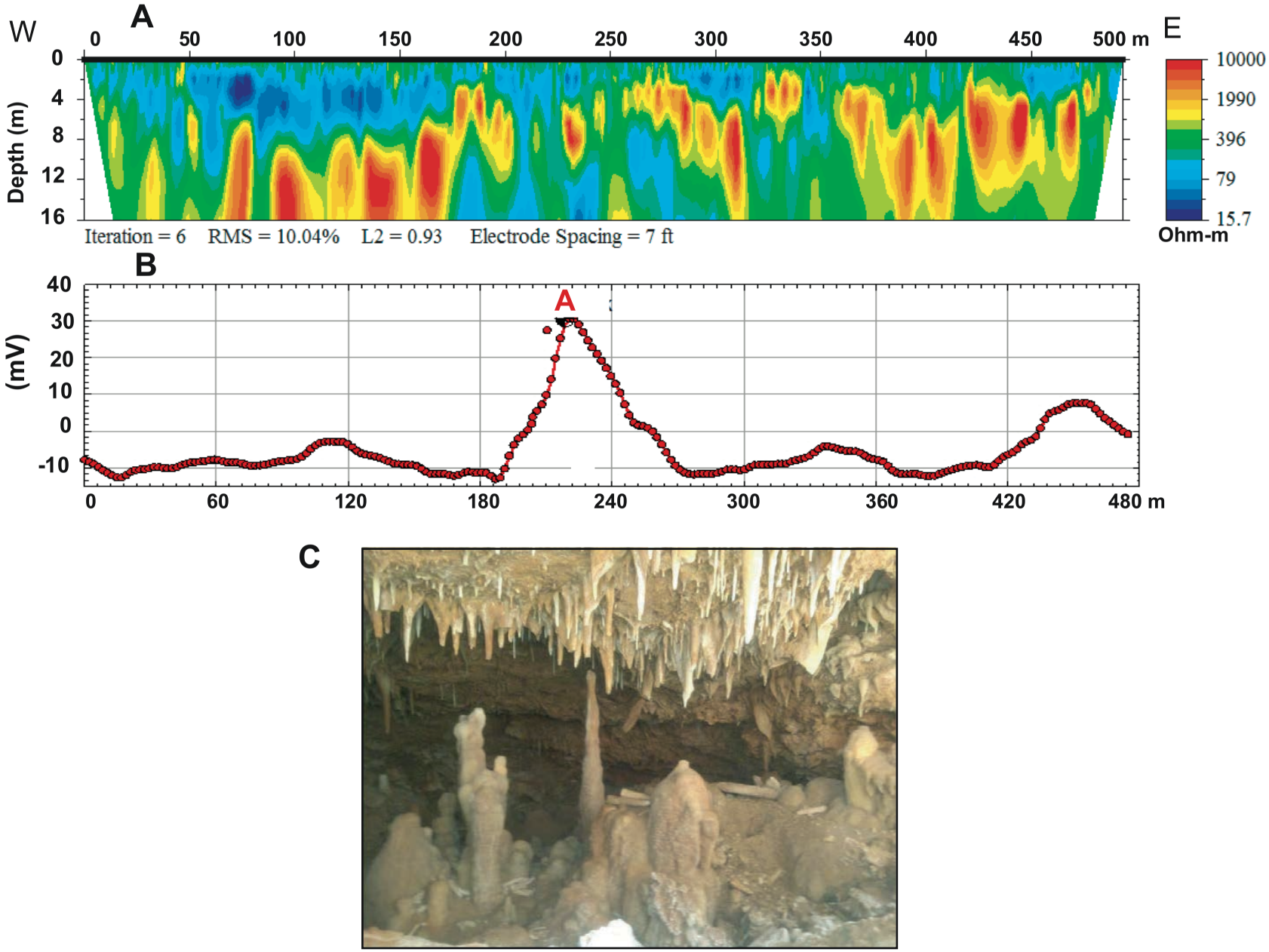

Figure 11. Geophysical survey results: (A) resistivity and (B) natural potential (NP) data in the southwestern part of the study area. (C) The cave encountered near NP anomaly A during the excavation for the Martin Hill Transmission Main. RMS error (root mean squared) in A is the statistical parameter that gives a difference between measured and calculated resistivity values. Scale is unknown for C. 7 ft = 2 m.

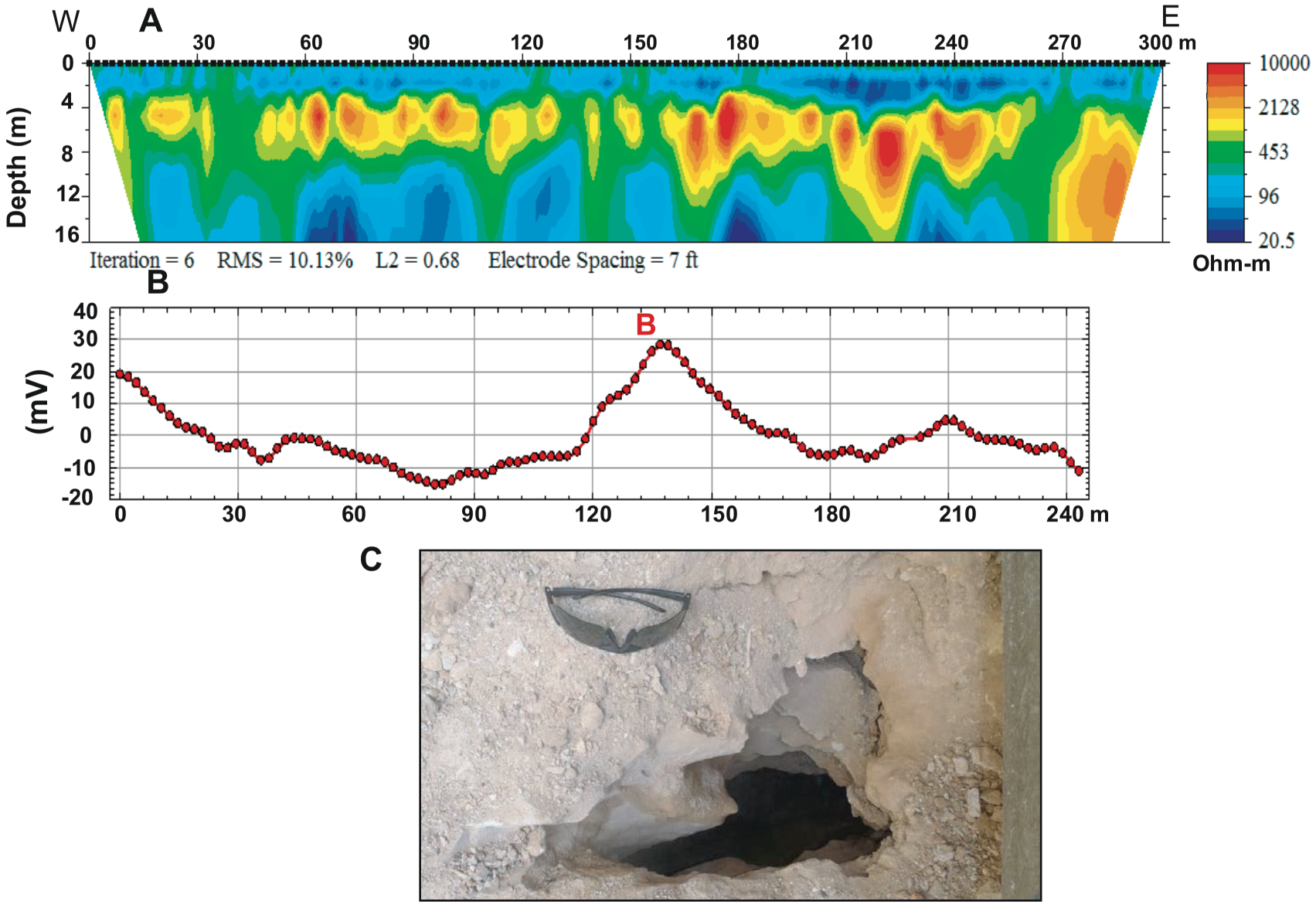

Figure 12. Geophysical survey results: (A) resistivity and (B) natural potential (NP) data in the southwestern part of the study area. (C) The cave encountered near NP anomaly A during the excavation for the Martin Hill Transmission Main. RMS error (root mean squared) is the statistical parameter that gives a difference between measured and calculated resistivity values. 7 ft = 2 m.

paper like this is a journey from the past, and I am grateful to the many people who helped me along the way. Thanks go to Art Lange, my mentor on the natural potential method, who has been instrumental in helping me to understand the natural potential technique and apply it correctly in the field. I dedicate this paper to him. Special thanks go to Alfred Hawkins, who has been my associate since late 1990s, for his help for all those years, sharing the load of the fieldwork with me, and having a good time … most of the time. I would like to thank Nico Hauwert of City of Austin, for being very supportive and providing up-to-date geological information on some of the data that are presented in this paper. Last, but not least, I would like to thank reviewers, in alphabetical order, R. Green, T. Halihan, M. Lagmanson, and J. Sharp for their insightful comments.

REFERENCES CITED

Blome, C.D., Smith, B.D., Smith, D.V., Faith, J.R., Hunt, A.G., Moore, D.W., Miggins, D.P., Ozuna, G.P., and Landis, G.P., 2008, Multidisciplinary studies of the Edwards Aquifer and adjacent Trinity Aquifer of south-central Texas: American Association of Petroleum Geologists Search and Discovery Article 80018 (adapted from oral presentation at AAPG Annual Convention), http://pubs.usgs.gov/fs/2006/3145.

Clark, A.K., 2000, Vulnerability of Ground Water to Contamination, Edwards Aquifer Recharge Zone, Bexar County, Texas, 1998: U.S. Geological Survey Water-Resources Investigation Report 00-4149, 9 p., 1 sheet.

Connor, C.B., and Sandberg, S.K., 2001, Application of integrated geophysical techniques to characterize the Edwards Aquifer, Texas: South Texas Geological Society Bulletin, v. 41, no. 7, p. 11–25.

Ferrill, D.A., and Morris, A.P., 2008, Fault zone deformation controlled by carbonate mechanical stratigraphy, Balcones fault system, Texas: American Association of Petroleum Geologists Bulletin, v. 92, no. 3, p. 359–380, https://doi.org/10.1306/10290707066.

Fitterman, D.V., and Stewart, M.T., 1986, Transient electromagnetic sounding for groundwater: Geophysics, v. 51, no. 4, p. 995–1005, https://doi.org/10.1190/1.1442158.

Gary, M.O., Rucker, D.F., Smith, B.D., Smith, D.V., and Befus, K., 2013, Geophysical investigations of the Edwards-Trinity Aquifer system at multiple scales: Interpreting airborne and direct current resistivity in karst, *in* 13th Sinkhole Conference/National Cave and Karst Research Institute (NCKRI) Symposium 2: National Cave and Karst Research Institute, p. 195–206, https://doi.org/10.5038/9780979542275.1127.

Green, R.T., Miller, M., McGinnis, R., Prikryl, J., and Morales, M., 2015, Integration of multiple 3D electrical resistivity surveys to evaluate the presence of karst features, *in* 28th Symposium on the Application of Geophysics to Engineering and Environmental Problems, 22–26 March: San Antonio, Texas, p. 391.

Hauwert, N.M., 2009, Groundwater Flow and Recharge within the Barton Springs Segment of the Edwards Aquifer, Southern Travis and Northern Hays Counties, Texas [Ph.D. dissertation]: Austin, Texas, University of Texas, 328 p.

Hauwert, N.M., Johns, D., Hunt, B., Beery, J., Smith, B., and Sharp, J.M., 2004, Flow systems of the Edwards Aquifer Barton Springs segment interpreted from tracing and associated field studies, *in* Howarka, S., ed., Edwards Water Resources in Central Texas, Retrospective and Prospective Symposium Proceedings: San Antonio, Texas, South Texas Geological Society and Austin Geological Society, 18 p.

Lindgren, R.J., Dutton, A.R., Hovorka, S.D., Worthington, S.R.H., and Painter, S., 2004, Conceptualization and Simulation of the Edwards Aquifer, San Antonio Region, Texas: U.S. Geological Survey Scientific Investigations Report 2004-5277, p. 122–130.

Maclay, R.W., and Land, L.F., 1988, Simulation of Flow in the Edwards Aquifer, San Antonio Region, Texas, and Refinements of Storage and Flow Concepts: U.S. Geological Survey Report Water-Supply Paper 2336-A, 48 p.

Musgrove, M., and Banner, J.L., 2004, Controls on the spatial and temporal variability of vadose drip water geochemistry: Edwards Aquifer, central Texas: Geochimica et Cosmochimica Acta, v. 68, no. 5, p. 1007–1020, https://doi.org/10.1016/j.gca.2003.08.014.

Prikryl, J.D., McGinnis, R.N., and Green, R.T., 2007, Evaluation of three-dimensional electrical resistivity array types for optimal detection of voids in karstic limestone, *in* Proceedings of the 2007 Symposium on the Application of Geophysics to Engineering and Environmental Problems (SAGEEP) Conference (extended abstract).

Saribudak, M., 2011, Urban geophysics: Geophysical signatures of Mt. Bonnell fault and its karstic features, Austin, Texas: Houston Geological Society Bulletin, v. 54, p. 49–54.

Saribudak, M., 2015, The million dollar question: Which geophysical methods locate caves best over the Edwards Aquifer? A potpourri of case studies from San Antonio and Austin, Texas, USA, *in* 14th Sinkhole Conference/National Cave and Karst Research Institute (NCKRI) Symposium 5: National Cave and Karst Research Institute, p. 355–364.

Saribudak, M., 2016, Geophysical mapping of Mount Bonnell fault of Balcones fault zone and its implications on Trinity-Edwards Aquifer interconnection, central Texas, USA: The Leading Edge, v. 35, no. 9, p. 752–758.

Saribudak, M., and Hauwert, N.W., 2017, Integrated geophysical investigations of Main Barton Springs, Austin, Texas, USA: Journal of Applied Geophysics, v. 138, p. 114–126, https://doi.org/10.1016/j.jappgeo.2017.01.004.

Saribudak, M., Hawkins, A., Saraiva, K., Terez, J., and Stoker, K., 2010 Geophysical signature of Haby Crossing fault and its implication on Edwards recharge zone, Medina County, Texas, *in* Long, J., ed., Contribution to the Geology of South Texas: San Antonio, Texas, South Texas Geological Society, p. 321–328.

Saribudak, M., Hawkins, A., and Stoker, K., 2012a, Do air-filled caves cause high resistivity anomalies? A six-case study from the Edwards Aquifer recharge zone in San Antonio, Texas: Houston Geological Society Bulletin, v. 54, no. 9, p. 41–49.

Saribudak, M., Hunt, B., and Smith, B., 2012b, Resistivity imaging and natural potential applications to the Antioch fault zone in the Onion Creek/Barton Springs segment of the Edwards Aquifer, *in* Gulf Coast Association of Geological Societies 62nd Annual Convention: Gulf Coast Association of Geological Societies Transactions, v. 62, p. 411–421.

Saribudak, M., Hauwert, N.W., and Hawkins, A., 2013, Geophysical signatures of Barton Springs (Parthenia, Zenobia and Eliza) of the Edwards Aquifer, Austin, Texas, *in* 12th Sinkhole Conference Proceedings: Carbonates and Evaporites, v. 28, no. 1–2, p. 75–87, https://doi.org/10.1007/s13146-013-0155-4.

Shah, S.D., Smith, B.D., Clark, A.K., and Payne, J.D., 2008, An Integrated Hydrogeologic and Geophysical Investigation to Characterize the Hydrostratigraphy of the Edwards Aquifer in an Area of Northeastern Bexar County, Texas: U.S. Geological Survey Scientific Investigations Report 2008-5181, 26 p., https://doi.org/10.3133/sir20085181.

Small, T.A., and Clark, A.K., 2000, Geologic Framework and Hydrogeologic Characteristics of the Edwards Aquifer Outcrop, Medina County, Texas: U.S. Geological Survey Water-Resources Investigation Report 00-4195, 10 p., 1 sheet.

Smith, B.D., Cain, M.J., Clark, A.K., Moore, D.W., Faith, J.R., and Hill, P.L., 2005, Helicopter Electromagnetic and Magnetic Survey Data and Maps, Northern Bexar County: U.S. Geological Survey Open-File Report 2005-1158, 122 p.

Stein, W.G., and Ozuna, G.B., 1996, Geologic Framework and Hydrogeologic Characteristics of the Edwards Aquifer Recharge Zone, Bexar County, Texas: U.S. Geological Survey Water-Resources Investigation Report 95-4030, scale 1:75,000, 8 p., 1 plate.

Manuscript Accepted by the Society 14 February 2019
Manuscript Published Online 8 July 2019